

4D objects-by-change

Spatiotemporal segmentation of geomorphic surface change from LiDAR time series

Anders, Katharina; Winiwarter, Lukas; Lindenbergh, Roderik; Williams, Jack G.; Vos, Sander E.; Höfle, Bernhard

DOI

[10.1016/j.isprsjprs.2019.11.025](https://doi.org/10.1016/j.isprsjprs.2019.11.025)

Publication date

2020

Document Version

Final published version

Published in

ISPRS Journal of Photogrammetry and Remote Sensing

Citation (APA)

Anders, K., Winiwarter, L., Lindenbergh, R., Williams, J. G., Vos, S. E., & Höfle, B. (2020). 4D objects-by-change: Spatiotemporal segmentation of geomorphic surface change from LiDAR time series. *ISPRS Journal of Photogrammetry and Remote Sensing*, 159, 352-363.
<https://doi.org/10.1016/j.isprsjprs.2019.11.025>

Important note

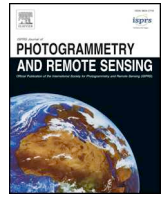
To cite this publication, please use the final published version (if applicable).
Please check the document version above.

Copyright

Other than for strictly personal use, it is not permitted to download, forward or distribute the text or part of it, without the consent of the author(s) and/or copyright holder(s), unless the work is under an open content license such as Creative Commons.

Takedown policy

Please contact us and provide details if you believe this document breaches copyrights.
We will remove access to the work immediately and investigate your claim.



4D objects-by-change: Spatiotemporal segmentation of geomorphic surface change from LiDAR time series

Katharina Anders^{a,b,*}, Lukas Winiwarter^a, Roderik Lindenbergh^c, Jack G. Williams^a, Sander E. Vos^d, Bernhard Höfle^{a,b,e}

^a 3D Geospatial Data Processing Group (3DGeo), Institute of Geography, Heidelberg University, 69120 Heidelberg, Germany

^b Interdisciplinary Center for Scientific Computing (IWR), Heidelberg University, 69120 Heidelberg, Germany

^c Department of Geoscience & Remote Sensing, Delft University of Technology, the Netherlands

^d Department of Hydraulic Engineering, Delft University of Technology, the Netherlands

^e Heidelberg Center for the Environment (HCE), Heidelberg University, 69120 Heidelberg, Germany

ARTICLE INFO

Keywords:

Terrestrial laser scanning
High-frequency observation
Spatiotemporal analysis
Beach monitoring
Temporal domain

ABSTRACT

Time series of topographic data are becoming increasingly widespread for monitoring geomorphic activity. Dense 3D time series are now obtained by near-continuous terrestrial laser scanning (TLS) installations, which acquire data at high frequency (e.g. hourly) and over long periods. Such datasets contain valuable information on topographic evolution over varying spatial and temporal scales. Current analyses however are mostly conducted based on pairwise surface or object-based change, which typically require the selection of thresholds and intervals to identify the processes involved and fail to account for the full history of change. Detected change may therefore be difficult to attribute to one or more underlying geomorphic processes causing the surface alteration. We present an automatic method for 4D change analysis that includes the temporal domain by using the history of surface change to extract the period and spatial extent of changes. A 3D space-time array of surface change values is derived from an hourly TLS time series acquired at a sandy beach over five months (2967 point clouds). Change point detection is performed in the time series at individual locations and used to identify change processes, such as the appearance and disappearance of an accumulation form. These provide the seed to spatially segment '4D objects-by-change' using a metric of time series similarity in a region growing approach. Results are compared to pairwise surface change for three selected cases of anthropogenic and natural processes on the beach. The obtained information reflects the evolution of a change process and its spatial extent over the change period, thereby improving upon the results of pairwise analysis. The method allows the detection and spatiotemporal delineation of even subtle changes induced by sand transport on the surface. 4D objects-by-change can therefore provide new insights on spatiotemporal characteristics of geomorphic activity, particularly in settings of continuous surfaces with dynamic morphologies.

1. Introduction

Earth surface morphology is continually shaped by dynamic processes. Induced surface changes within a natural landscape occur at varying locations and at different spatial scales, frequencies, and movement rates. Monitoring of geomorphic activity therefore requires the observation of a multitude of individual, often superimposed processes. Alterations to surface morphology are often quantified based on the distance between surface locations recorded at successive points in time, referred to as epochs in geospatial analysis (Eitel et al., 2016; Lindenbergh and Pietrzyk, 2015). At present, such change analyses are

mostly conducted as pairwise comparisons, referring to the quantification of change between two epochs. Pairwise analysis involves the drawback that change information is obtained as an aggregated representation of individual underlying processes. When observed as local surface changes at single points in space and between only two snapshots of the topography, it is not possible to infer which process led to the current state of the surface and how it evolved through time. At the same time, the underlying change is not necessarily distinguishable into deposition, erosion, and transport without ambiguity (Fig. 1). Relating quantified local surface change to the processes that shaped the surface is therefore a widespread challenge in the analysis of

* Corresponding author at: 3DGeo at the Institute of Geography, Im Neuenheimer Feld 368, 69120 Heidelberg, Germany.

E-mail addresses: katharina.anders@uni-heidelberg.de (K. Anders), lukas.winiwarter@uni-heidelberg.de (L. Winiwarter), R.C.Lindenbergh@tudelft.nl (R. Lindenbergh), jack.williams@uni-heidelberg.de (J.G. Williams), s.e.vos@tudelft.nl (S.E. Vos), hoefle@uni-heidelberg.de (B. Höfle).

<https://doi.org/10.1016/j.isprsjprs.2019.11.025>

Received 4 October 2019; Received in revised form 27 November 2019; Accepted 27 November 2019

Available online 09 December 2019

0924-2716/ © 2019 International Society for Photogrammetry and Remote Sensing, Inc. (ISPRS). Published by Elsevier B.V. All rights reserved.

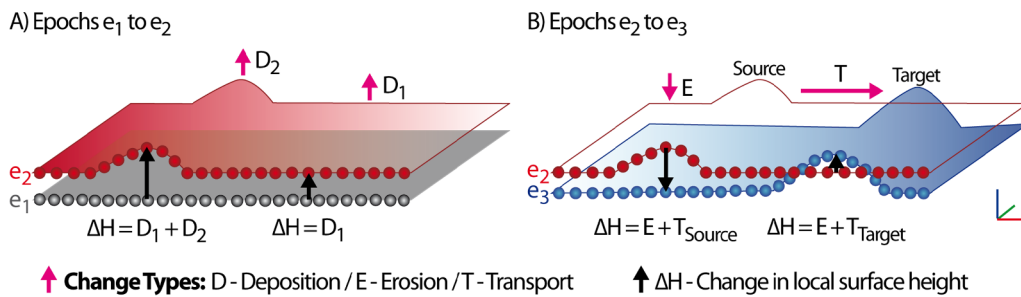


Fig. 1. Pairwise observation of change types ‘deposition’, ‘erosion’, and ‘transport’ co-occurring in a geomorphic system. The processes that underlie single values of local surface height change are ambiguous. (A) Observed change can result from superimposed surface alterations (e.g. D_1 and D_2). The spatial extent of accumulation form D_2 on the continuous surface is not distinct. (B) Local surface height decrease at the source of transported material and increase at the target location cannot be attributed unambiguously to the respective change types erosion E and transport T.

geomorphic activity (Fey et al., 2019; Mayr et al., 2018).

Analysing time series of geospatial data has the potential to increase insight into the mechanisms of geomorphic activity (Eltner et al., 2017; O’Dea et al., 2019). This study focuses on the morphodynamics of a sandy beach, where sediment transport is driven by an interplay of agents, including wind and wave forcing, as well as anthropogenic modifications. The resulting multi-process characteristics of periodic, gradual and continual change processes occurring at different time scales apply to a range of natural topographies, including rock slopes (Kromer et al., 2015a), glaciers (Rossini et al., 2018), rock glaciers (Zahs et al., 2019) or permafrost coasts (Obu et al., 2017). The observation of individual change processes and analysis of their contribution to the geomorphic system requires data acquired at spatial and temporal resolutions that account for the range of scales at which the induced changes occur (Rumson et al., 2019).

As the research on and the variety of applications of geospatial monitoring grow, more series of multitemporal data are being acquired at repetition rates that are annual, monthly, or even shorter (Eitel et al., 2016) with a range of topographic survey techniques. High-frequency (sub-hourly to weekly repetition intervals) time series of high spatial resolution (sub-centimetre to metre) and long acquisition periods (months to years) are becoming increasingly available through near-continuous terrestrial laser scanning (TLS; e.g. Kromer et al., 2017; O’Dea et al., 2019; Vos et al., 2017; Williams et al., 2018).

While datasets are being captured at increasing temporal resolution, methods for analysing surface change from geospatial time series mostly follow the described approach of pairwise analysis of local surface changes. This approach is well-established in analysing conventional multitemporal LiDAR data of several epochs (typically < 100; e.g., Corbí et al., 2018; Fey et al., 2019; Mayr et al., 2018; Zahs et al., 2019). Pairwise analyses are also suitable in settings where surface change is progressing in a more or less uniform direction, i.e. deposition or erosion is the dominant change type, and the effect on surface morphology is irreversible. This applies, for example, in the case of continuous erosion on a slope or rockfall on a cliff (e.g. Kromer et al., 2017; Williams et al., 2018). In such settings, the possible change processes are mostly known a priori and pairwise surface change can be attributed to the respective (expected) process.

An alternative approach to surface change quantification is object-based geomorphic change analysis (Anders et al., 2013; Liu et al., 2010). These methods quantify the surface or volume change and displacement of individual geomorphic features or objects within a scene. Such features are extracted from each epoch of the multitemporal data and are typically based on morphometric properties, such as breaks in curvature at edges or planar surfaces on objects. The approach is used, for example, to monitor the change of characteristic units or structures on beaches (Corbí et al., 2018; Fabbri et al., 2017; Le Mauff et al., 2018) or the displacement of breaklines as geomorphic features, representing scarps or ridges (Mayr et al., 2018; Pfeiffer et al., 2018). The required identification and classification of objects typically implies the

definition of morphometric properties for target objects from the outset. This becomes particularly challenging when monitoring over long periods, where features can occur in many variations of their spatial properties. It also requires that objects can be spatially delineated within each epoch, which is only possible if they have a distinct morphology. In the flat and gently sloping surface morphology of a sandy beach, for example, the exact spatial extent of an accumulation form is difficult to determine even to a human observer both on site and in high-resolution topographic data.

Binary surface change information (change/no change) between successive epochs has been considered for the spatial delineation of objects in the segmentation of morphometric features (Mayr et al., 2017). Change objects are defined as spatially connected areas of pairwise change, which has been introduced into coastal monitoring (Liu et al., 2010). If such object-based assessment considers change between only two epochs, the spatial boundary of individual change types may remain concealed by coinciding surface alterations caused by multiple processes. For example, localised accumulations within an area of large-scale accretion will be aggregated into a single change object of combined extent. The spatial and temporal properties of the processes involved, however, often differ over time. Accretion is a slow, continual process while local accumulation may occur more rapidly and, from this, become distinct in the evolution of surface change at the location. This additional information that can be gained from the temporal domain, and in particular the history of change of each point on the surface is difficult to integrate into the interpretation of change for a given location at a single, specific point in time. The identification of objects therefore requires the entire history of change of a given point on the surface.

Our research develops a novel approach to 4D (3D + time) change analysis that fully incorporates the temporal domain, with the aim of improving the identification of change processes in time series of geospatial data. We make use of the full available history of surface change for the purpose of spatiotemporal object segmentation, in doing so advancing the concept of pairwise change objects to ‘4D objects-by-change’. Spatial neighbourhoods that experience similar surface change within certain periods are delineated based on their similarity in the temporal domain. This removes the requirement of object detection and re-identification in single or pairwise snapshots and removes the need of having a strict definition of object in terms of temporal processes or morphometric properties, such as size and shape. Integrating time series into surface change analysis allows the inclusion of a variety of spatial and temporal scales (extent, magnitude and duration) in the identification of geomorphic change. A metric of time series similarity integrates flexibility of spatial extent in object extraction. Otherwise, spatial delineation of change may mainly depend on the definition of threshold values even if object boundaries are difficult to determine conceptually.

Our method provides a novel view on time series-based surface change analysis, which allows automatic and generic extraction of the

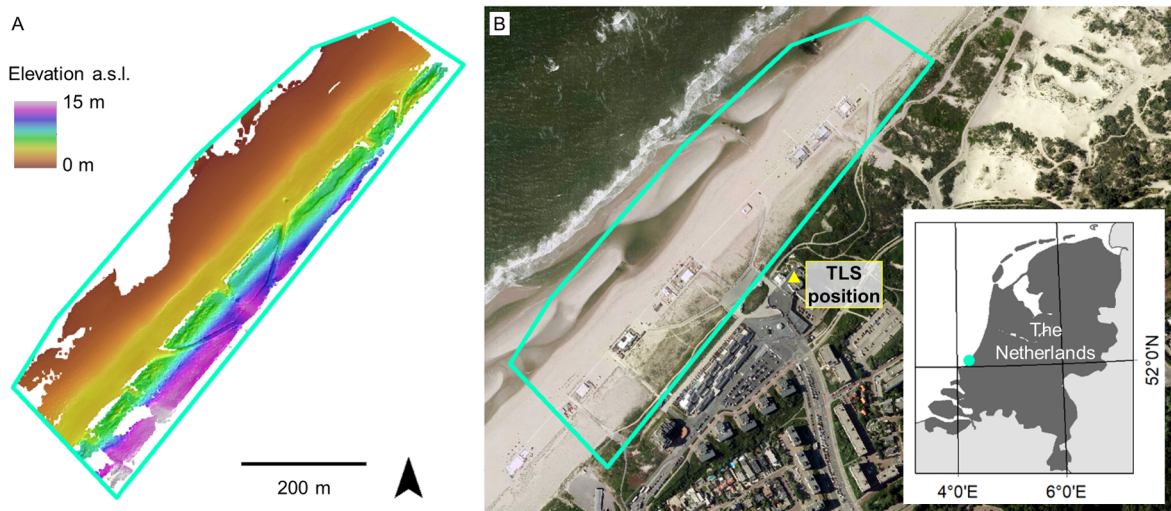


Fig. 2. (A) Terrain elevation of the study site (based on TLS data) with extent designated in (B) aerial imagery of the beach at Kijkduin with map of the study site location in the Netherlands. Data: Aerial imagery © pdok.nl 2017, World Borders © thematicmapping.org 2017.

4D geoinformation present in time series of 3D topographic data. 4D objects-by-change generate more detailed histories of identified surface change as compared to pairwise surface change analysis. This will provide a basis for relating individually identified change types to specific geographic processes, and to assess their contribution to the dynamic shaping of a landscape.

2. Study site and data

We present our method using a time series of 3D point clouds acquired at the sandy beach of Kijkduin ($52^{\circ}04'14''\text{N}$, $4^{\circ}13'10''\text{E}$; Fig. 2), the Netherlands. A Riegl VZ-2000 TLS (Riegl LMS, 2017) was mounted in a stable reference frame overlooking the beach during the winter of 2016–2017 (Vos et al., 2017). The scene was scanned every hour with a vertical and horizontal point spacing of 9 mm at 10 m measurement range. The target area of the beach ranges between 100 and 600 m from the sensor resulting in point densities of 2–20 points/m².

The period examined starts on 2017-01-15 at 13:00 (Central European Time; UTC + 1), following a storm event in the days before, and ends on 2017-05-26 at 8:00, which is the end date of the fixed TLS acquisition at this site. Several epochs are missing due to rainfall that prevented any data from being acquired at the measurement range of the target area. In total, the time series comprises 2967 point clouds. Gaps in local areas of an epoch may exist due to missing data in the respective point cloud caused by occlusion of the ground surface (e.g. temporary objects such as machinery and people) or the presence of water on the surface (e.g. at high tides) during scan acquisitions.

Pre-processing of the TLS data consists of fine alignment of each point cloud to a global reference point cloud of the first day (2017-01-15, 15:00). This fine alignment is conducted with an Iterative Closest Point method (Besl and McKay, 1992). The alignment accuracy is assessed based on point-to-plane distances for planar surfaces distributed in the stable region of the point cloud scene, which are distinct from the surfaces used for fine alignment. The method of fine alignment and the determination of alignment accuracy are described in detail in Anders et al. (2019). The pre-processed TLS time series has a mean alignment accuracy of 4 mm with a standard deviation of 2 mm. The minimum detectable change is further limited due to a range-dependent refraction effect in the LiDAR measurements that varies over time with atmospheric conditions (cf. Friedli et al., 2019). At the measurement range of the beach area, the minimum detectable change is estimated to reach up to 0.05 m (cf. Anders et al., 2019). The temporally dense measurements of the dataset can be leveraged to reduce

uncertainty from the quantified change. We make use of this in a temporal averaging step (Section 3.1). Each point cloud is filtered to remove off-terrain points based on the relative height of points over the local minimum in a neighbourhood of 1.0 m raster cells. The filtering threshold is set to a maximum relative height of 0.2 m to account for surface roughness and the slightly sloping terrain morphology. We use the software OPALS (Pfeifer et al., 2014) for the pre-processing steps of fine alignment and terrain filtering. This time series of pre-processed point clouds is used for all subsequent analyses in this paper.

3. Methods

For the extraction of 4D objects-by-change, we develop a method of spatial segmentation with respect to the history of surface change. The method identifies change processes as temporal features within the time series of surface change. The features include both raising of the surface followed by lowering and lowering of the surface followed by raising. The locations are used in a regular grid structure, derived from point cloud distances per epoch. Local neighbourhoods are then spatially grown into 4D objects-by-change based on the similarity of time series segments (Fig. 3). The methodological steps are presented in detail in the following sub-sections (Sections 3.1, 3.2 and 3.3). We evaluate the results of our approach in comparison to the current standard procedure of pairwise, binary threshold-based analysis (Section 3.4), which provides single images of surface change between two epochs instead of the full history of surface change contained in our approach.

3.1. Deriving a space-time array of surface change

For the developed approach, the time series of 3D point clouds is processed into a time series of surface change in a regular grid structure. Re-sampling into this 3D space-time array of surface change values facilitates data access along the temporal domain.

We quantify surface change on the beach as the vertical distance of the surface between each epoch and a reference point cloud on the first day of the analysed period (2017-01-15, 13:00). The epoch at this time of day was selected due to the low tide, enabling measurements over a large extent of the beach area. Point cloud distances are derived using the Multiscale Model to Model Cloud Comparison (M3C2) algorithm (Lague et al., 2013). We use a regular grid with 0.5 m horizontal spacing to define the 2D locations at which distances between the two point clouds are calculated. This spacing is chosen regarding the lowest point spacing in the target scene (Section 2). The projection radius

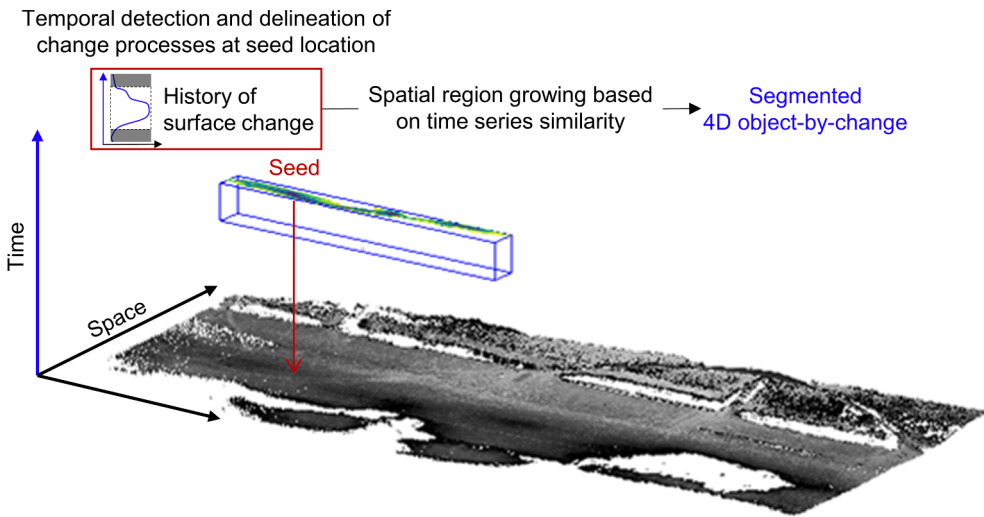


Fig. 3. Approach for the extraction of 4D objects-by-change. A change process is detected and delineated in the time series of surface change at one location. The temporal change feature is used as seed for spatial region growing. The homogeneity criterion for region growing is the similarity of time series in the period of the temporal change feature. The segmented 4D object-by-change has a temporal and spatial extent in the space-time array.

(Lague et al., 2013), representing the neighbourhood within which the position of each point cloud is averaged during distance calculation, was set to 1.0 m. The distance calculation at the regular grid locations uses all original TLS points within the projection radius.

Using the obtained space-time array of surface change, we perform averaging of the surface change values for every 2D point location on the beach along the temporal domain, i.e. based on the values at previous and successive points in time. This enables the identification of values that notably deviate from their temporal neighbours and are less likely to represent actual change rather than measurement errors in the point cloud. Each surface change value in the time series of a location is averaged by setting it to the median of its temporal neighbourhood in a window of defined size. The approach benefits from sampling redundancy in the temporal domain particularly if the acquisition frequency exceeds the rate of observed surface change. Accordingly, the averaging window needs to be sufficiently small to avoid smoothing out the temporal trend of the actual surface change (Kromer et al., 2015b). We use a temporal averaging window of one week (168 h) on the beach data in this study. This offers a compromise between removing temporal measurement effects from variable atmospheric conditions (Anders et al., 2019) and preserving morphologic change, providing an interdependent combination of exceeding the minimum detectable change (in terms of magnitude) and the temporal scale (in terms of duration).

3.2. Identification of temporal change features

Our approach to 4D change analysis begins by identifying the occurrence of a change-inducing process in the time series of change values (Fig. 4). We first determine the points in time at which the height change values in the time series change with respect to the mean. These

change points are used to delineate change features in the temporal domain based on the shape of the time series.

Change point detection can be performed by comparing the distribution of values between two successive periods, i.e. segments of the time series. The instants at which this relationship changes are to be detected as change points (Kawahara and Sugiyama, 2012; Truong et al., 2019). Segments are derived based on changes in the median of the change values, i.e. the central point of the value distribution within a segment, with least absolute deviation as measure of homogeneity (Bai, 1995; Truong et al., 2019). The change point detection method uses a sliding temporal window to compute the discrepancy between two adjacent windows that move along the signal. This sliding temporal window is subsequently referred to as change point detection window. Peaks in the discrepancy curve determine the position of change points (Truong et al., 2019). As the number of change points to be detected is unknown in our application, a constraint needs to be introduced for dividing the time series into increasingly small segments. We use a complexity penalty in the time series segmentation which acts in relation to the amplitude (i.e. magnitude) of changes to detect. The higher the penalization, the stricter the change point detection. Conversely, the lower the penalization value, the more change points are detected down to discrepancies that derive from noise in the signal (Maidstone et al., 2017; Truong et al., 2019).

We use a change point detection window of 24 h, considering that change values are smoothed in an averaging window of one week (Section 3.1). This ensures that the smallest temporal scale of change occurrences that are contained in the time series dataset are detected. We set the penalty for change point detection to 1.0, such that the number of detected change points does not strongly alter with an increase or decrease of the penalty. The step size of the change point detection window is 1 h, so change points can potentially be detected at

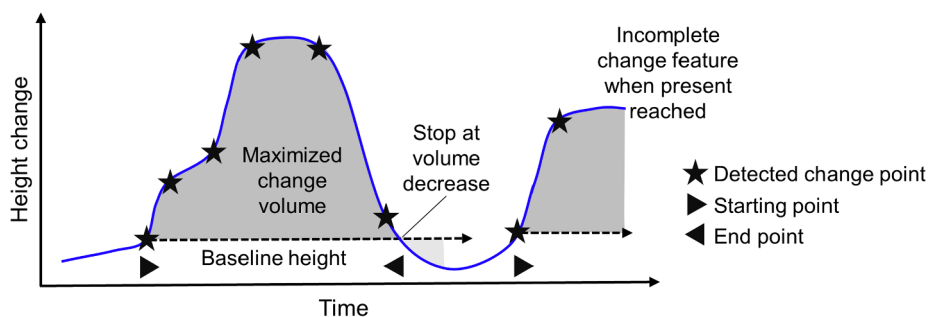


Fig. 4. Schematic representation of temporal change feature delineation using the earliest change point that is not within a previous change feature as a starting point. The end point is increased as long as the volume of surface change (area under the curve) increases with respect to the starting point's change value as baseline.

each epoch of the time series. We constrain the change point detection by setting a minimum distance of 12 h between change points so that there is no overlap between temporal windows of detected change points. The change point detection is performed using the implementation in the Python library *ruptures* (Truong et al., 2018).

Change processes are identified within the time series of surface elevation change by using a normalised volume maximization approach to identify their start and end times (Piltz et al., 2016). From a detected change point as starting point, the change feature is grown along the temporal axis by increasing the time of the end point for as long as the area under the curve of surface change values is increasing. The increase or decrease of the change volume is determined relative to the value of the starting point as baseline. In the process, the cumulative surface change of the change feature is maximized. As soon as adding another epoch of surface change has the effect of decreasing this cumulative value, the process is stopped (Fig. 4). This step is applied to all change points detected in the time series, starting from the earliest. Successive change points are only used as new starting points if they do not lie within a previously detected change feature. By this, over-sensitively detected change points are automatically discarded. To be able to delineate both positive and negative change features, we include a check if the surface change in epochs following the starting point is negative (relative to the starting point). For negative features, the time series is inverted so the same procedure of delineation can be applied. All time series are shifted to contain only positive values for this step. Once a change feature is delineated in the temporal domain of a location, the next step is to segment the 4D object-by-change spatially based on neighbouring locations of similar temporal change features.

3.3. Spatial segmentation of 4D objects-by-change

We assume that geomorphic change at a given location causes similar surface alterations within a local neighbourhood. We use this to group spatially contiguous locations with a similar history of surface change in the period of a temporal change feature. In a region growing approach, an area is segmented based on the similarity of neighbouring time series as homogeneity criterion (Fig. 5), to form a 4D object-by-change.

For the period of features derived in Section 3.2, we derive the similarity of the time series for each point in the grid using Dynamic Time Warping (DTW, Berndt and Clifford, 1994). This method finds the alignment between two time series by stretching and shrinking a reference time series along the temporal domain. The sum of minimized distances between point pairs in the time series yields the DTW distance as a similarity measure (Berndt and Clifford, 1994; Salvador and Chan, 2007). We subtract the median value from each input time series segment for this calculation to assess the time series similarity independent from the previous history of surface change. As surface change is quantified using a fixed epoch as reference, this history may differ between neighbouring locations but they still belong to the same 4D object-by-change. We compute the DTW distance using the implementation of the Fast DTW algorithm (Salvador and Chan 2007) in the Python library *fastdtw* (Tanida, 2019).

The spatial region growing starts at a seed location by computing the DTW distance to all eight connected spatial neighbours of the 2D time series locations. If the distance of a compared location exceeds a defined similarity threshold, it is discarded. Otherwise, the similar locations are added to the current segment. We use a stricter, but adaptive criterion of using a segmented location as a new search location based on the distribution of distance values in the current segment. A location for searching further spatial neighbours as candidates is added if the DTW distance of the segmented location is smaller than the 95th percentile of all distance values segmented so far (Rabbani et al., 2006). The percentile threshold of adding candidates as additional search locations initiates when the segment reaches a minimum segment size of 10, corresponding to an area of ~2.5 m² for the dataset in this study. Before this segment size is reached, all segmented locations are used as neighbour search locations. After checking all neighbours of a current search location, the candidate with the lowest DTW distance is used. The growing of a segment is stopped when no more search locations are available.

For the segmentation threshold, there is no single DTW distance that can be used as general similarity value, as the order of DTW distance values between two time series that are regarded as similar relate to the overall change energy, i.e. the total surface height changes within the process, as well as magnitude and duration of the respective change

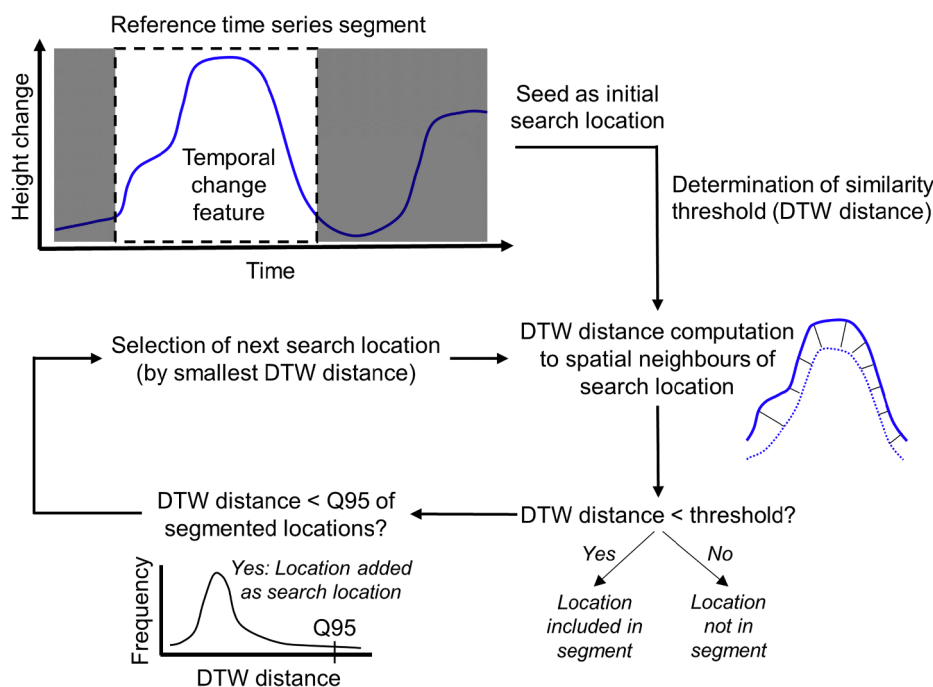


Fig. 5. Spatial segmentation of a 4D object-by-change starting from the location of the detected temporal change feature as seed and computing the Dynamic Time Warping (DTW) distance as similarity criterion for adding locations to the segment and using them as additional search locations for region growing.

process. We therefore selected a threshold by assessing the distribution of DTW values within the 10×10 m neighbourhood of initial seeds. According to the results of this assessment, we set the threshold to the mean of DTW distance values.

3.4. Test cases and comparison to pairwise surface change analysis

To evaluate the time series-based change analysis compared to results from simple pairwise analysis, we pick representative cases of change processes with different spatial and temporal properties to examine the improvement in information obtained from the 4D approach. The following cases are selected from the acquisition period at the Kijkduin beach scene:

- (1) An accumulation of sand that was later removed by heavy machinery. The change has a high magnitude (> 1.5 m surface height increase) and is limited to a small spatial extent ($\sim 4 \times 4$ m). Both accumulation and removal of the sand occur quickly relative to the time interval of monitoring.
- (2) A sand bar that forms and later disappears near the shoreline. The sand bar has a high magnitude of change (> 0.8 m) but does not have distinct spatial borders (Section 1) as it translates and deforms over time.
- (3) A mass of sand transported towards the upper beach area on destruction of the sand bar. The resulting temporary surface height increase (> 0.15 m) is well above the minimum detectable change but only subtly visible in the topography, which makes it difficult to spatially delineate.

For comparison to a pairwise analysis, we use individual 2D slices from the 3D space-time array, which represent pairwise surface height change of an epoch to the reference epoch. These change rasters are derived from the epochs in the beginning and end of a segmented 4D object-by-change, and at the highest magnitude of surface change within the period of the change process.

4. Results

In this section, we present the results of the change feature delineation and spatial segmentation based on time series similarity. We then present the extracted 4D object-by-change of selected cases as compared to pairwise surface change.

4.1. Identification of temporal change features

The examples of change described in Section 3.4 were detected from the time series of surface change (Fig. 6). Additional change features were detected in the time series of cases 1 and 3. In case 3, the second change feature is not completed with an end point, as the time series ends before completion.

The method for change point detection accurately delineates the periods of change in the selected cases. These cases show that the spatial scale and temporal pattern of surface change does not influence the delineation of the targeted features. The placement of starting and

end points in the change features may not provide the optimal positions to determine the onset and end of a change process for all types. For example, the starting point of accumulation in a change feature may be set at a point after surface height increase of the process has already started (Fig. 6, case 1). This does not influence the extraction of 4D object-by-change, but can become relevant to subsequent analyses, for example to quantify the contribution of individual change processes to the volume budget in the geomorphic system.

For the dataset at hand, we perform retrospective change point detection, that is, all data has been collected and the full time series is processed. As we use a window-based approach that can continuously advance into the future independently from past occurrences, the method can be applied in an operational, online setting to detect change processes as soon as possible after or even while they occur.

4.2. Spatial segmentation of 4D object-by-change

We show the result for the three selected cases as time series plots of all segmented locations within the period of the change feature, and the spatial extent on the beach area (Fig. 7). We additionally show the distribution of DTW distance values, which altogether provides a visual summary of the information contained in a 4D object-by-change.

The time series plots (Fig. 7, subfigures A) show the constellation of (i) the temporal course of surface change values and (ii) the spatial scale of surface change values within the segment. The skewness in the distribution of DTW distance values (Fig. 7, subfigures B) expresses the characteristics of continuous change of the sandy surface. Starting from a central seed location of high magnitude in a local elevation maximum, the similarity will gradually decrease mainly with increasing spatial distance. Limiting the region growing into space by the percentile threshold of adding new search locations (Section 3.3) provides a suitable means of constraining the segmentation.

The decisive factor in the spatial delineation of 4D objects-by-change is the parametrization of the segmentation, i.e. the selection of a suitable DTW distance threshold for adding locations to the segment. The segmentation threshold influences the strictness in the spatial delineation of change processes. A larger threshold increases the spatial extent of a segmented change object, which is expressed in the distribution of DTW distance values, i.e. similarities in the history of surface change over time. However, no definition of spatial object boundaries for individual change processes is required. A variation of similarities within the area of a 4D object-by-change represents the degree of vagueness in its spatial extent.

The spatial extents resulting for the selected cases show that the determination of the DTW distance threshold is independent of the spatial scale of a change process. Both a small area (case 1) and larger areas (cases 2 and 3) with different ranges of DTW distance values are spatially delineated (Fig. 7, subfigures C). Automatic parametrization is important for the application of the approach in operational geomorphic monitoring, where multiple process types can be detected. The transferability of the parameter determination method to other types of change processes and use cases requires investigation.

The spatial segmentation of the different change processes for the selected cases is compared to pairwise surface change in the following

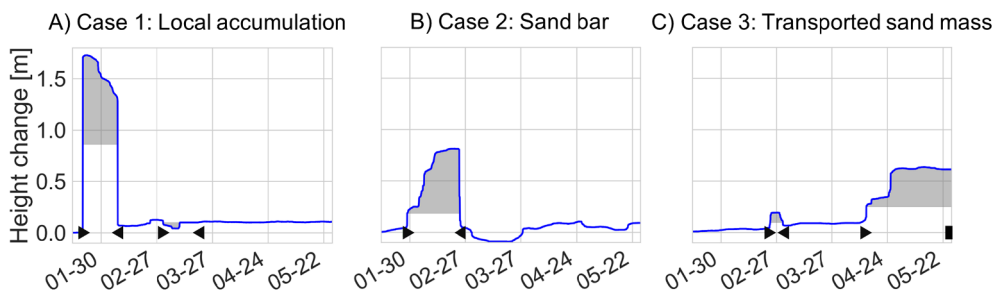


Fig. 6. Result of temporal change feature delineation for the selected cases of (A) an accumulation of sand shifted by heavy machinery works, (B) a sand bar forming and disappearing near the shoreline, and (C) a mass of sand being transported that is manifested in local surface height increase and decrease at the selected location. Starting and end point of change features are marked by triangles. Dates are provided as month-day.

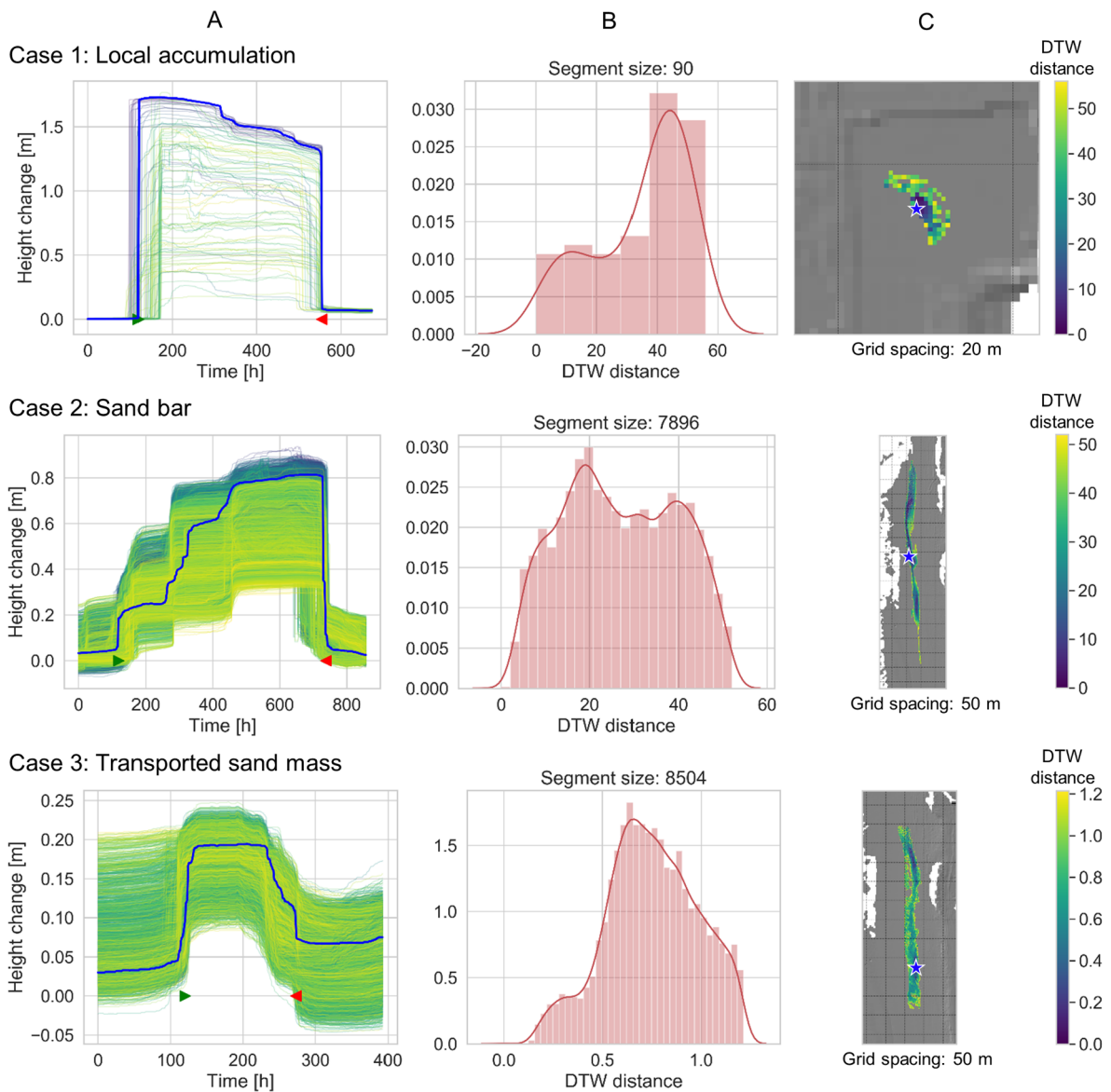


Fig. 7. 4D object-by-change for three example cases resulting from region growing segmentation based on Dynamic Time Warping (DTW) distance as time series similarity in the period of a temporal change feature at a seed location. (A) Time series of all 2D locations included in the segment coloured by DTW distance, with the reference time series (in blue) as seed location marked with star in (C) overview map. (B) Distribution of DTW distances in the segment with Gaussian kernel density estimate. (For interpretation of the references to colour in this figure legend, the reader is referred to the web version of this article.)

section and shows how the 4D objects-by-change in our use case represent the change forms.

4.3. Evaluation of 4D objects-by-change in relation to pairwise change detection

In this section we compare the results obtained from the pairwise analysis to the 4D objects-by-change. Animated visualizations are provided to illustrate the temporal evolution of surface change reflected in the time series segments of respective 4D objects-by-change (Supplements I-III).

The sand accumulation shifted by heavy machinery (case 1) is a case of surface change that is easily identifiable in the pairwise change detection as a spatially contiguous area of surface change increase. Our approach is able to extract the change process at least as well in its spatial extent (Fig. 8).

In comparison to the pairwise surface change analysis, the 4D objects-by-change provides additional information on the detected change

process, such as its temporal evolution. It becomes apparent that the accumulation occurred rapidly and only little material was removed or shifted subsequently (Fig. 8A). From the simultaneous appearance and disappearance in the time series at all locations within the 4D object-by-change, we can deduce that it is a local accumulation form and no movement of the sand body occurred.

The sand bar (case 2) is a natural accumulation that is visible in the topography but is not easily detected in the surface change data, as its spatial extent is difficult to define quantitatively. The segmented 4D object-by-change presents the spatial extent of the form with increasing vagueness towards the borders, while the elongated core area shows high inner-segment similarity regarding the time series of surface change during existence of the sand bar (Fig. 9B).

The pairwise raster of the sand bar shows a state where the change object becomes distinguishable as a high-magnitude accumulation object (Fig. 9C, 2017–02–21). However, the visible pattern in the course of time series segments indicates that the sand bar deformed. Further, the sand bar moved over the time of its existence. This becomes visible

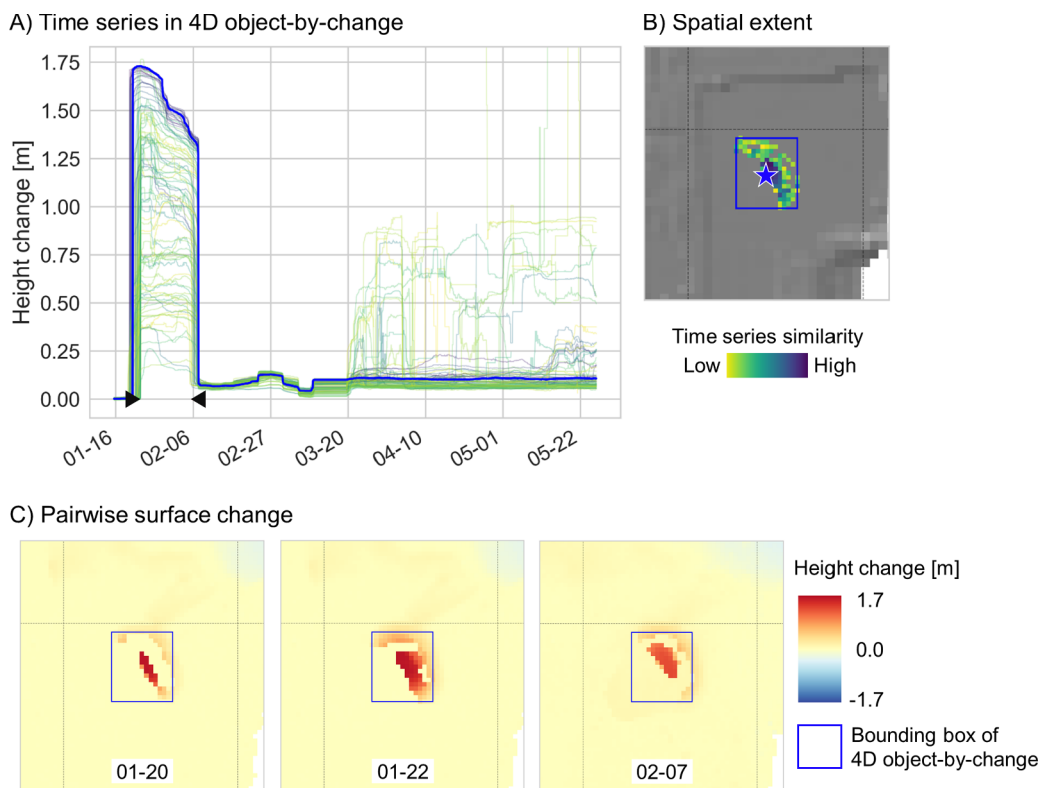


Fig. 8. 4D object-by-change extracted for an accumulation of sand built up and removed by heavy machinery (case 1). (A) Time series of all 2D locations included in the segment coloured by the similarity metric (Dynamic Time Warping distance). (B) Spatial extent and location of the reference time series (seed location, marked by star). (C) Rasters of pairwise surface height change at the start, maximum magnitude, and end of the temporal change feature compared to the first epoch of the time series. Start and end are marked by the triangles in the time series plot (A). Axes grid has a spacing of 20 m.

in the animation of pairwise surface change, where the sand body is shifted in the bounding box of the 4D object-by-change (Supplement II). The 4D change analysis therefore provides a more comprehensive assessment on the spatial extent of the sand bar than individual epochs of positive surface height change.

This aspect is advanced with the third case of sand material transported on destruction of a sand bar. This is only subtly manifested in the areal surface change, although it is well-delineable in the time series at individual locations (Fig. 10A). The relevance of considering the temporal domain for identifying this change process becomes particularly evident here. The change does not appear as distinctly delineable in the pairwise surface change and would likely not be identified from such analysis. Particularly in contrast to the surrounding higher magnitude changes, the surface change is hardly identifiable in individual rasters as spatially contiguous, delimited area of an individual change process (Fig. 10C). With this, time series-based change analysis improves the detection of change processes. To illustrate the representation of the change process in the combined spatial and temporal domain, we refer to the animation provided in Supplement III.

5. Discussion

At present, standard approaches to geospatial change analysis are based on pairwise comparison between epochs. In multi-process geomorphic settings, this will often lead to quantified surface change being ambiguous to the underlying geomorphic change. Observed change can then not be linked to individual change processes.

5.1. Improvement over pairwise surface change and implications for geomorphic analyses

Existing methods of pairwise surface and object-based change analysis mostly require epochs to be selected for change quantification and thresholds to be set to detect and delineate observed objects and changes, which is typically based on their morphometric parameters. This requirement is difficult to meet on continuous surfaces, as given by

the morphology of sandy beaches. Beach morphology and changes therein have conventionally been examined using surface elevation profiles (Smith and Zarillo, 1990), with multitemporal LiDAR being used to supplement these data in recent years (e.g. Miles et al., 2019; Stockdon et al., 2009; van Houwelingen et al., 2006). Accumulation forms, such as sand bars, can be localised in profiles based on their crests, and troughs in between, and their migration can be detected from the displacement of crests in repeatedly sampled profiles (Cohn et al., 2018; Levoy et al., 2013; Miles et al., 2019, Reichmuth and Anthony, 2008). This approach is convenient as the shaping and migration of forms is mainly wave-driven in a cross-shore direction. Sampling of parallel cross-shore profiles accounts for long-shore variability in beach morphology (Grunnet and Hoekstra, 2004; Masselink and Anthony, 2001). However, it has become evident that more comprehensive consideration of 3D morphology is required, for example, to understand the evolution of bar systems from their individual width and volume (Miles et al., 2019). LiDAR data provide high-resolution 3D morphology of surfaces, yet describing morphologic forms from these data requires an approach for spatial delineation. When analysing the evolution of change forms, our method enables delineation directly in the spatial domain by making use of the surface change history, removing the need to localise morphometric parameters as is done in terrain profiles. Obtained 4D objects-by-change provide a basis for analysing the spatial properties of extracted forms.

In addition to improved spatial delineation, we obtain information regarding the evolution of the surface for all change types delineated in a 4D object-by-change in drawing upon the temporal domain. The temporal evolution of surface change can be used to interpret detected change processes. Considering the representative cases of morphologic change on the beach shown in this paper, cases 2 and 3 in particular require change evolution as information to deduce the types of geomorphic activity involved. The transport of a sand mass given in case 3 does not become evident in either the spatial or temporal domain. If considered as image of pairwise surface change, the process would likely be interpreted as overall accretion on the surface within the spatial domain. Considering the time series of surface change at a single

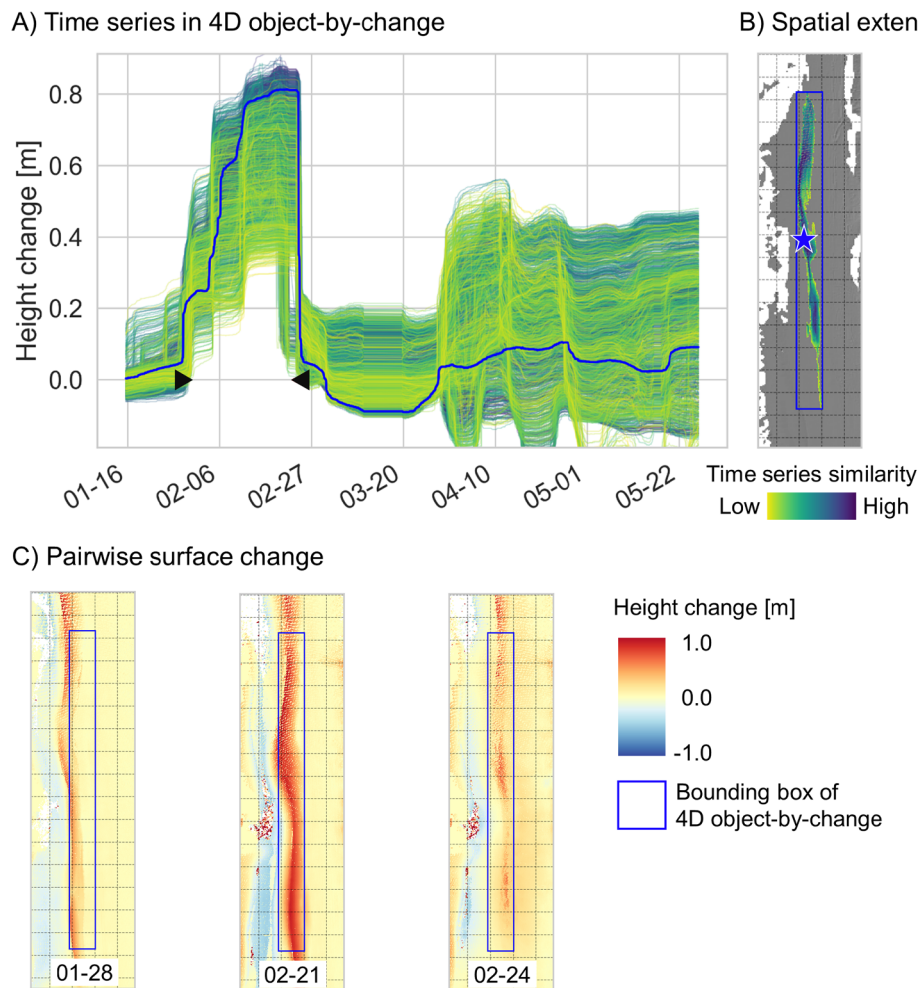


Fig. 9. 4D object-by-change extracted for a sand bar (case 2). (A) Time series of all 2D locations included in the segment coloured by the similarity metric (Dynamic Time Warping distance). (B) Spatial extent and location of the reference time series (seed location, marked by star). (C) Rasters of pairwise surface height change at the start, maximum magnitude, and end of the temporal change feature compared to the first epoch of the time series. Start and end are marked by the triangles in the time series plot (A). Axes grid has a spacing of 50 m.

location, the change process may represent local accumulation and disappearance of material, formed naturally or by anthropogenic modification as in case 1. These aspects highlight the enhanced level of information given by a 4D object-by-change. The method uses this information in combining the spatial and temporal domains for spatio-temporal delineation, while current methods consider smaller subsets of data (pairwise) or information (only spatial or temporal domains). The further interpretation of identified and extracted change processes holds potential for improved comprehensiveness in the analysis and interpretation of geomorphic activity, for example by linking the transported sand mass as consequence to the destruction of a sand bar. Identifying and understanding relations between change processes is an important task in geomorphology, which is supported by our method. A prominent example is the detection of pre-failure deformation leading up to a rockfall event (Kromer et al., 2017; Royán et al., 2014). By spatially segmenting the area affected by pre-failure deformation using our method, the spatiotemporal properties of the resulting 4D object-by-change can provide information on the mechanisms of failure evolution. The detection of precursors to geomorphic change events and their spatiotemporal delineation represents an opportunity to apply our method, which can be integrated to increase the understanding of geomorphic process dependencies and the realization of early warning systems in hazard management (cf. Abellán et al., 2016).

The ability to detect and delineate increasingly subtle change forms is a useful addition to the interpretation of change. We show this in our

use case with the example of a mass of sediment being transported on destruction of a sand bar (case 3). Time series-based surface change analysis enables the capture of transient forms, which are important features of temporary sediment mobility particularly in the context of aeolian sand transport (Nield et al., 2011). Such short-term mobility and resulting displacement of sand mass was identified from linear trends in surface height change by de Vries et al. (2017) using short-term sub-hourly TLS time series acquired in a beach plot. Applying the extraction of 4D objects-by-change to the time series data could provide additional information on the behaviour of mobilised sand in this setting. Similar to case 3 in this paper, migrating features would be delineated as individual objects and can be separated from locations that are subject to local erosion or accumulation only. By delineating change forms spatiotemporally, our approach enables to decouple them from other potentially overlapping changes, such as longer-term overall accretion on the beach co-occurring with the transient change form of case 3.

5.2. Methodological considerations for 4D objects-by-change

We present the detection and delineation of surface change acting bidirectionally on a location, such as the formation and disappearing of an accumulation form (cases 1 and 2) or the transient form of a transported sand mass that appears in local surface change only temporarily (case 3). The methodological aspect to be highlighted here is

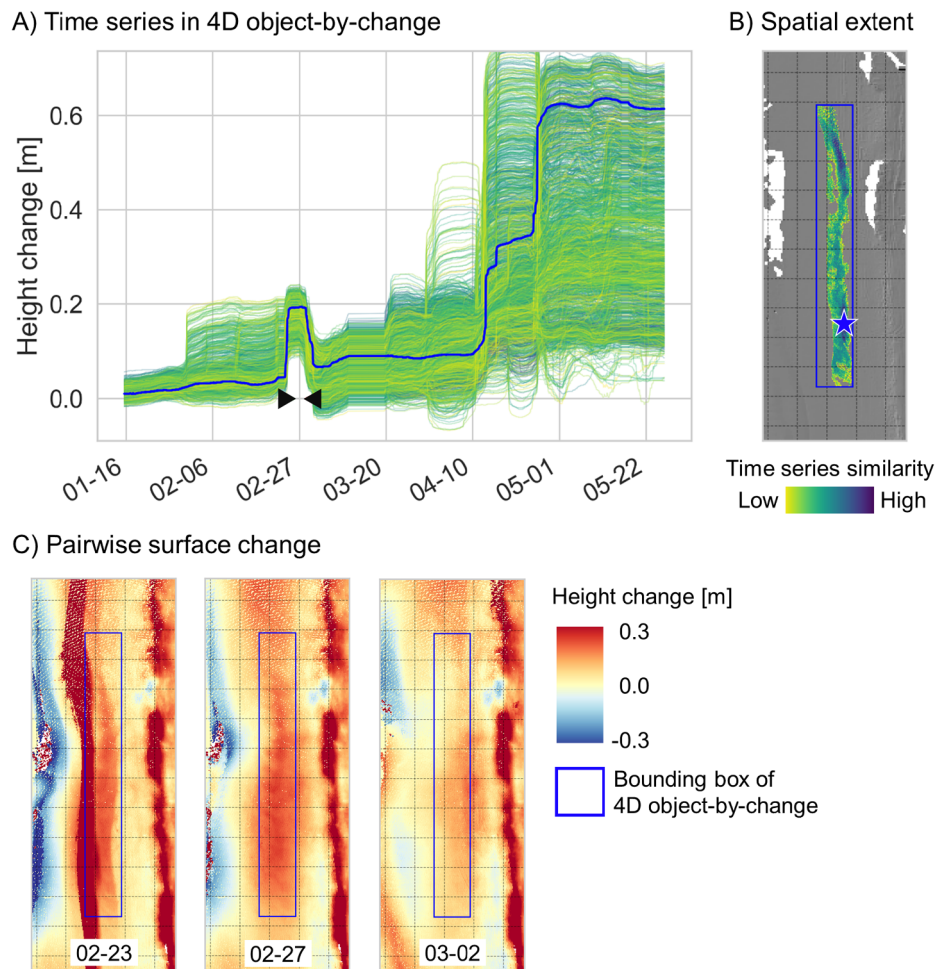


Fig. 10. 4D object-by-change extracted for a form expressed through sand transport (case 3). (A) Time series of all 2D locations included in the segment coloured by the similarity metric (Dynamic Time Warping distance). (B) Spatial extent and location of the reference time series (seed location, marked by star). (C) Rasters of pairwise surface height change at the start, maximum magnitude, and stop of the temporal change feature compared to the first epoch of the time series. Start and stop are marked by the triangles in the time series plot (A). Axes grid has a spacing of 50 m.

that the temporal delineation of bidirectional change is independent from the temporal scale, i.e. definitions of timing and duration of a change process. Given a topographic time series, bidirectional change can therefore be captured and considered in the analysis of volume change in a geomorphic system. The effect of such changes being lost to the observation was highlighted in Anders et al. (2019), where observed volume change on a sandy beach was reduced by a factor of five if temporary accumulation forms, such as the existence of a sandbar over few weeks, are not included in the analyses. The application of our method is not necessarily exclusive to surface change values, as it may also be used directly upon time series of gridded elevation data (e.g. Digital Elevation Models) and then does not require a decision on the reference epoch. The strength of our approach and previously outlined improvements over current approaches of surface change analysis apply particularly in geomorphic settings where material is deformed and transported over predominantly continuous surface morphology.

While focusing on the detection of bidirectional change which characterises complex geomorphic settings, the temporal change delineation in our presented method can be extended to include further geomorphic change types. Generically, this regards the identification of unidirectional changes such as erosion being permanent after a discrete event or on conclusion of a continual change process. This will require application-dependent definitions of when a change is considered permanent to conclude a change process, such as continuous surface height increase through accretion on the beach. Discrete events on the beach

can be erosion induced by heavy storms, which often interrupt continual processes (O’Dea et al., 2019). While time series-based surface change analysis thereby provides an approach for comprehensive observation of geomorphic activity in multi-process systems, it might be less useful to replace current approaches in settings where morphologic change occurs predominantly unidirectionally and event-driven. For example, in rockfall monitoring on a coastal cliff – in contrast to rockfall events embedded in the multi-process setting of an active landslide – discrete events are distinctly identifiable in the three-dimensional surface morphology and their volume can be quantified from pairwise comparison of the pre- and post-event state of the surface (Williams et al., 2018). For general applicability to the analysis of geomorphic activity, we expect our method to be useful as soon as the temporal sampling of the topographic data exceeds the movement rate of change, i.e. the transition from the initial to the altered surface morphology is represented in several epochs of the time series. To what temporal resolution the time series can be reduced for different change types and use cases will require investigation.

In addition to the spatial and temporal properties of a surface change process, the spatial-temporal grouping of time series segments provides a new information layer given in the similarity metric of DTW distance. Grouping change processes extracted from large geospatial time series builds the basis for identifying patterns, such as periodicity in the timing of occurrence or spatial-temporal sequences of change types. For example, sand bar evolution can be investigated on the level

of single objects, but also regarding patterns of migration within the system for different object types (cf. Section 5.1). For this, the inner-segment distribution of similarities provides an attribute for semantic classification of process types for a number of objects, even generically where not all occurrences are known. This renders the approach advantageous also for change analysis where the delineation of areas or objects underlying morphologic change is distinct and defined. Where spatial boundaries are not definite, the distribution of DTW distances in the area of an identified change process reflects extensional uncertainty, for example in case of decreasing similarity towards the spatial boundary of an object. This vagueness in the spatial extent of objects has been subject to research particularly for the case of sandy beaches (Molenaar and Cheng, 2000; Stein et al., 2004). When handling geomorphic objects or change forms as vague spatial objects (Dilo et al., 2007), DTW distances could be used as quantification of vagueness provided in a 4D object-by-change.

6. Conclusion

We have presented a technique to extract 4D objects-by-change using time series-based change analysis of natural surfaces within settings of spatially and temporally variable change. The approach improves the level of information that can be gained from time series of topographic data compared to standard pairwise analysis. It enables the detection of processes of change over a range of timescales and without requiring a selection of epochs to use for surface change quantification. Change forms are spatially delineated, which is independent of thresholds that are typically required for extracting objects from epochs of surface change. The extracted 4D objects-by-change provide information on the characteristics of change processes with detailed histories of identified surface change that are present in geospatial time series. Several fields of application are discussed where the method can improve change analysis and provide new insights on spatiotemporal properties of geomorphic activity. This methodological advancement is particularly relevant in light of the growing availability of time series data both through continued survey repetitions and increasing numbers of near-continuous TLS acquisitions at increased temporal resolution.

Declaration of Competing Interest

The authors declare that they have no known competing financial interests or personal relationships that could have appeared to influence the work reported in this paper.

Acknowledgements

This work was supported in part by the Heidelberg Graduate School of Mathematical and Computational Methods for the Sciences (HGS MathComp), founded by DFG grant GSC 220 in the German Universities Excellence Initiative. We thank two anonymous reviewers for their comments, which helped improve the manuscript. Data acquisition was performed within the CoastScan project and financed by the European Research Council [ERC Advanced Grant 291206, Nearshore Monitoring and Modeling (NEMO)].

The funding sources had no role in the research design, analysis and interpretation of data, and the writing and decision to submit the article for publication.

Appendix A. Supplementary material

Supplementary data to this article can be found online at <https://doi.org/10.1016/j.isprsjprs.2019.11.025>.

References

Abellán, A., Derron, M.-H., Jaboyedoff, M., 2016. "Use of 3D Point clouds in geohazards"

- special issue: current challenges and future trends. *Remote Sens.* 8 (2). <https://doi.org/10.3390/rs8020130>.
- Anders, K., Lindenbergh, R.C., Vos, S.E., Mara, H., de Vries, S., Höfle, B., 2019. High-frequency 3D geomorphic observation using hourly terrestrial laser scanning data of a sandy beach. *ISPRS Ann. Photogram., Remote Sens. Spatial Inf. Sci.* IV-2/W5, 317–324. <https://doi.org/10.5194/isprs-annals-IV-2-W5-317-2019>.
- Anders, N.S., Seijmonsbergen, A.C., Bouten, W., 2013. Geomorphological change detection using object-based feature extraction from multi-temporal LiDAR data. *IEEE Geosci. Remote Sens. Lett.* 10 (6), 1587–1591. <https://doi.org/10.1109/LGRS.2013.2262317>.
- Bai, J., 1995. Least absolute deviation of a shift. *Econometric Theory* 11, 403–436.
- Berndt, D.J., Clifford, J., 1994. Using dynamic time warping to find patterns in time series. *AAAI-94 Workshop on Knowledge Discovery in Databases*, 10(16), 359–370.
- Besl, P., McKay, N., 1992. A method for registration of 3-D shapes. *IEEE Trans. PAMI* 14 (2), 239–256.
- Cohn, N., Ruggiero, P., de Vries, S., Kaminsky, G.M., 2018. New insights on coastal foredune growth: the relative contributions of marine and aeolian processes. *Geophys. Res. Lett.* 45 (10), 4965–4973. <https://doi.org/10.1029/2018gl077836>.
- Corbí, H., Riquelme, A., Megías-Baños, C., Abellan, A., 2018. 3-D morphological change analysis of a beach with seagrass berm using a terrestrial laser scanner. *ISPRS Int. J. Geo-Inf.* 7 (234), 15. <https://doi.org/10.3390/ijgi7070234>.
- de Vries, S., Verheijen, A., Hoonhout, B., Vos, S., Cohn, N., Ruggiero, P., 2017. Measured spatial variability of beach erosion due to aeolian processes. *Proc. Coastal Dynamics* 2017 (71), 481–491.
- Dilo, A., de By, R.A., Stein, A., 2007. A system of types and operators for handling vague spatial objects. *Int. J. Geogr. Inf. Sci.* 21 (4), 397–426. <https://doi.org/10.1080/13658810601037096>.
- Eitel, J.U.H., Höfle, B., Vierling, L.A., Abellán, A., Asner, G.P., Deems, J.S., Glennie, C.L., Joerg, P.C., LeWinter, A.L., Magney, T.S., Mandlbürger, G., Morton, D.C., Müller, J., Vierling, K.T., 2016. Beyond 3-D: The new spectrum of lidar applications for earth and ecological sciences. *Remote Sens. Environ.* 186, 372–392. <https://doi.org/10.1016/j.rse.2016.08.018>.
- Eltner, A., Kaiser, A., Abellan, A., Schindewolf, M., 2017. Time lapse structure-from-motion photogrammetry for continuous geomorphic monitoring. *Earth Surf. Proc. Land.* 42, 2240–2253. <https://doi.org/10.1002/esp.4178>.
- Fabbri, S., Giambastiani, B.M.S., Sistilli, F., Scarelli, F., Gabbianelli, G., 2017. Geomorphological analysis and classification of foredune ridges based on Terrestrial Laser Scanning (TLS) technology. *Geomorphology* 295, 436–451. <https://doi.org/10.1016/j.geomorph.2017.08.003>.
- Fey, C., Schattan, P., Helfricht, K., Schöber, J., 2019. A compilation of multi-temporal TLS snow depth distribution maps at the Weisssee snow research site (Kauernalpe, Austria). *Water Resour. Res.* 55 (6), 5154–5164. <https://doi.org/10.1029/2019wr024788>.
- Friedli, E., Presl, R., Wieser, A., 2019. Influence of atmospheric refraction on terrestrial laser scanning at long range. In: *Proceedings of the 4th Joint International Symposium on Deformation Monitoring: JISDM, Athens, Greece*, pp. 6.
- Grunnet, N.M., Hoekstra, P., 2004. Alongshore variability of the multiple barred coast of Terschelling, The Netherlands. *Marine Geol.* 203 (1), 23–41. [https://doi.org/10.1016/S0025-3227\(03\)00336-0](https://doi.org/10.1016/S0025-3227(03)00336-0).
- Kawahara, Y., Sugiyama, M., 2012. Sequential change-point detection based on direct density-ratio estimation. *Stat. Anal. Data Min.: ASA Data Sci. J.* 5 (2), 114–127. <https://doi.org/10.1002/sam.10124>.
- Kromer, R.A., Abellán, A., Hutchinson, D., Lato, M., Edwards, T., Jaboyedoff, M., 2015a. A 4D filtering and calibration technique for small-scale point cloud change detection with a terrestrial laser scanner. *Remote Sens.* 7 (10), 13029–13052. <https://doi.org/10.3390/rs71013029>.
- Kromer, R.A., Hutchinson, D.J., Lato, M.J., Gauthier, D., Edwards, T., 2015b. Identifying rock slope failure precursors using LiDAR for transportation corridor hazard management. *Eng. Geol.* 195, 93–103. <https://doi.org/10.1016/j.enggeo.2015.05.012>.
- Kromer, R.A., Abellán, A., Hutchinson, D.J., Lato, M., Chanut, M.-A., Dubois, L., Jaboyedoff, M., 2017. Automated terrestrial laser scanning with near real-time change detection - monitoring of the Séchillenne landslide. *Earth Surf. Dyn.* 5, 293–310. <https://doi.org/10.5194/esurf-5-293-2017>.
- Lague, D., Brodu, N., Leroux, J., 2013. Accurate 3D comparison of complex topography with terrestrial laser scanner: application to the Rangitikei canyon (N-Z). *ISPRS J. Photogramm. Remote Sens.* 82, 10–26. <https://doi.org/10.1016/j.isprsjprs.2013.04.009>.
- Le Mauff, B., Juigner, M., Ba, A., Robin, M., Launeau, P., Fattal, P., 2018. Coastal monitoring solutions of the geomorphological response of beach-dune systems using multi-temporal LiDAR datasets (Vendée coast, France). *Geomorphology* 304, 121–140. <https://doi.org/10.1016/j.geomorph.2017.12.037>.
- Levoy, F., Anthony, E.J., Monfort, O., Robin, N., Bretel, P., 2013. Formation and migration of transverse bars along a tidal sandy coast deduced from multi-temporal LiDAR datasets. *Mar. Geol.* 342, 39–52. <https://doi.org/10.1016/j.margeo.2013.06.007>.
- Lindenbergh, R., Pietrzyk, P., 2015. Change detection and deformation analysis using static and mobile laser scanning. *Appl. Geomat.* 7 (2), 65–74. <https://doi.org/10.1007/s12518-014-0151-y>.
- Liu, H., Wang, L., Sherman, D., Gao, Y., Wu, Q., 2010. An object-based conceptual framework and computational method for representing and analyzing coastal morphological changes. *Int. J. Geogr. Inf. Sci.* 24 (7), 1015–1041. <https://doi.org/10.1080/13658810903270569>.
- Maidstone, R., Hocking, T., Rigai, G., Fearnhead, P., 2017. On optimal multiple change-point algorithms for large data. *Stat. Comput.* 27 (2), 519–533. <https://doi.org/10.1007/s11222-016-9636-3>.
- Masselink, G., Anthony, E.J., 2001. Location and height of intertidal bars on macrotidal ridge and runnel beaches. *Earth Surf. Proc. Land.* 26 (7), 759–774. <https://doi.org/10.1002/esp.220>.

- Mayr, A., Rutzinger, M., Bremer, M., Oude Elberink, S., Stumpf, F., Geitner, C., 2017. Object-based classification of terrestrial laser scanning point clouds for landslide monitoring. *Photogram. Rec.* 32 (160), 377–397. <https://doi.org/10.1111/phor.12215>.
- Mayr, A., Rutzinger, M., Geitner, C., 2018. Multitemporal analysis of objects in 3D point clouds for landslide monitoring. *Int. Arch. Photogram., Remote Sens. Spatial Inf. Sci. XLII-2*, 691–697. <https://doi.org/10.5194/isprs-archives-XLII-2-691-2018>.
- Miles, A., Ilic, S., Whyatt, D., James, M.R., 2019. Characterizing beach intertidal bar systems using multi-annual LiDAR data. *Earth Surf. Proc. Land.* 44 (8), 1572–1583. <https://doi.org/10.1002/esp.4594>.
- Molenaar, M., Cheng, T., 2000. Fuzzy spatial objects and their dynamics. *ISPRS J. Photogramm. Remote Sens.* 55 (3), 164–175. [https://doi.org/10.1016/S0924-2716\(00\)00017-4](https://doi.org/10.1016/S0924-2716(00)00017-4).
- Nield, J.M., Wiggs, G.F.S., Squirrell, R.S., 2011. Aeolian sand strip mobility and pro-dune development on a drying beach: examining surface moisture and surface roughness patterns measured by terrestrial laser scanning. *Earth Surf. Proc. Land.* 36 (4), 513–522. <https://doi.org/10.1002/esp.2071>.
- Obu, J., Lantuit, H., Grosse, G., Günther, F., Sachs, T., Helm, V., Fritz, M., 2017. Coastal erosion and mass wasting along the Canadian Beaufort Sea based on annual airborne LiDAR elevation data. *Geomorphology* 293, 331–346. <https://doi.org/10.1016/j.geomorph.2016.02.014>.
- O'Dea, A., Brodie, K.L., Hartzell, P., 2019. Continuous coastal monitoring with an automated terrestrial lidar scanner. *J. Marine Sci. Eng.* 7 (2), 37. <https://doi.org/10.3390/jmse7020037>.
- Pfeifer, N., Mandlbürger, G., Otepka, J., Karel, W., 2014. OPALS - A framework for Airborne Laser Scanning data analysis. *Comput. Environ. Urban Syst.* 45, 125–136. <https://doi.org/10.1016/j.compenvurbysys.2013.11.002>.
- Pfeiffer, J., Zieher, T., Bremer, M., Wichmann, V., Rutzinger, M., 2018. Derivation of three-dimensional displacement vectors from multi-temporal long-range terrestrial laser scanning at the reissenschuh landslide (Tyrol, Austria). *Remote Sens.* 10 (11), 1688.
- Piltz, B., Bayer, S., Poznanska, A.M., 2016. Volume based DTM generation from very high resolution photogrammetric DSMs. *Int. Arch. Photogramm. Remote Sens. Spatial Inf. Sci. XLI-B3*, 83–90. <https://doi.org/10.5194/isprs-archives-XLI-B3-83-2016>.
- Rabbani, T., Van Den Heuvel, F., Vosselmann, G., 2006. Segmentation of point clouds using smoothness constraint. *Int. Arch. Photogram., Remote Sens. Spatial Inf. Sci.* 36 (5), 248–253.
- Reichmuth, B., Anthony, E.J., 2008. Seasonal-scale morphological and dynamic characteristics of multiple intertidal bars. *Zeitschrift für Geomorphologie, Supplementary Issues* 52 (3), 79–90. <https://doi.org/10.1127/0372-8854/2008/0052S3-0079>.
- Riegl, L.M.S., 2017. Riegl VZ–2000 (datasheet). URL: https://www.3dlasermapping.com/wp-content/uploads/2017/10/DataSheet_VZ-2000_2017-06-07.pdf (11 Jan 2019).
- Rossini, M., Di Mauro, B., Garzonio, R., Baccolo, G., Cavallini, G., Mattavelli, M., De Amicis, M., Colombo, R., 2018. Rapid melting dynamics of an alpine glacier with repeated UAV photogrammetry. *Geomorphology* 304, 159–172. <https://doi.org/10.1016/j.geomorph.2017.12.039>.
- Royán, M.J., Abellán, A., Jaboyedoff, M., Vilaplana, J.M., Calvet, J., 2014. Spatio-temporal analysis of rockfall pre-failure deformation using Terrestrial LiDAR. *Landslides* 11 (4), 697–709. <https://doi.org/10.1007/s10346-013-0442-0>.
- Rumson, A.G., Hallett, S.H., Brewer, T.R., 2019. The application of data innovations to geomorphological impact analyses in coastal areas: An East Anglia, UK, case study. *Ocean Coast. Manag.*, 104875. <https://doi.org/10.1016/j.ocecoaman.2019.104875>.
- Salvador, S., Chan, P., 2007. Toward accurate dynamic time warping in linear time and space. *Intell. Data Anal.* 11 (5), 561–580. <https://doi.org/10.3233/IDA-2007-11508>.
- Smith, G.L., Zarillo, G.A., 1990. Calculating long-term shoreline recession rates using aerial photographic and beach profiling techniques. *J. Coastal Res.* 6 (1), 111–120.
- Stein, A., Dilo, A., Lucieer, A., van de Vlag, D., 2004. Definition and identification of vague spatial objects and their use in decision ontologies. In: *ISSDQ '04*, Bruck ad Leitha, Department of Geoinformation and Cartography, pp. 21.
- Stockdon, H.F., Doran, K. S., Jr., A. H. S., 2009. Extraction of Lidar-based dune-crest elevations for use in examining the vulnerability of beaches to inundation during hurricanes. *J. Coastal Res.* 59–65. doi: 10.2112/si53-007.1.
- Tanida, K., 2019. fastdtw – A Python implementation of FastDTW. URL: <https://github.com/slaypni/fastdtw> [version: 0.3.2] (28 June 2018).
- Truong, C., Oudre, L., Vayatis, N., 2018. ruptures: Change point detection in python. arXiv preprint: <https://arxiv.org/abs/1801.00826>.
- Truong, C., Oudre, L., Vayatis, N., 2019. A review of change point detection methods. arXiv preprint: <https://arxiv.org/abs/1801.00718>, pp. 46.
- van Houwelingen, S., Masselink, G., Bullard, J., 2006. Characteristics and dynamics of multiple intertidal bars, north Lincolnshire, England. *Earth Surf. Processes Landforms* 31 (4), 428–443. <https://doi.org/10.1002/esp.1276>.
- Vos, S., Lindenbergh, R., de Vries, S., 2017. CoastScan: continuous monitoring of coastal change using terrestrial laser scanning. *Proc. Coastal Dynamics 2017* (233), 1518–1528.
- Williams, J.G., Rosser, N.J., Hardy, R.J., Brain, M.J., Afana, A.A., 2018. Optimising 4-D surface change detection: an approach for capturing rockfall magnitude–frequency. *Earth Surf. Dyn.* 6, 101–119. <https://doi.org/10.5194/esurf-6-101-2018>.
- Zahs, V., Hämmerle, M., Anders, K., Hecht, S., Sailer, R., Rutzinger, M., Williams, J. G., Höfle, B. Multi-temporal 3D point cloud-based quantification and analysis of geomorphological activity at an alpine rock glacier using airborne and terrestrial LiDAR. *Permafrost Periglacial Processes*, 30(3), 222–238. doi: 10.1002/ppp.2004.